Some aspects on 2.5D true amplitude Kirchhoff common-angle time migration

Tânia M.G. Santiago* and Cláudio Guerra, *PETROBRAS*, Martin Tygel, *UNICAMP*

Summary

The analysis of amplitude variation with offset or reflection angle is of great importance in the oil industry to predict hydrocarbon presence in the reservoir. This analysis is applied to both reservoir and exploration areas. The usual transformation method from offset to reflection angle, for common-offset migrated data, involves errors that may produce unreliable results. Thus, it becomes necessary to find alternative procedures to obtain appropriate data to provide more reliable curves of amplitude versus reflection angle (AVA). This work considers 2.5D true amplitude Kirchhoff-time migration in the common-angle domain, and its application to synthetic seismic data. It also examines the influence of seismic acquisition and migration aperture on the migration results. Comparison between AVA curves obtained from common-angle and common-offset migrated data confirms that the former is a more reliable procedure.

Introduction

Recently, much attention has been paid in obtaining angle gathers during migration process. This can be performed using slant-stack and Fourier routines or, in the Kirchhoff migration basis, considering travel-time curves related to the common-angle configuration. Such procedures differ from the 1D traditional ones because these don't take into account reflector dips. Once time migration doesn't deal with multiple paths, the main advantage of the Kirchhoff common-angle time migration (KCATM) is to obtain more accurate AVA curves in steep dip areas.

Fomel and Prucha (1999) approach KCATM to introduce the angle-gather concept. They describe the travel-time curve and provide a true amplitude weighting function for KCATM.

In present paper, we describe this migration scheme providing a new true amplitude weighting function for the acoustic case. Additionally, we show how to parameterize the migration aperture to obtain true amplitudes. Synthetic examples prove this weighting function is correct.

Kirchhoff common-angle time migration

The 2.5D Kirchhoff common-angle time migration can be represented by the following integral along a certain travel-time curve, τ_D,

$$V(M) = \int_A da . W(a, M) D[U(a, t = t_D(a, M))]; \qquad (1)$$

where, $V(M)$ is the migrated common-angle domain output, a is the migration dip, $W(a,M)$ is a weighting function, D represents the half-derivative operator, $U(a,t)$ is the seismic data, represented by its analytical form, to be migrated and A is the migration aperture that defines the extension of the migration operator. If the amplitudes to locate in $V(M)$ are supposed to represent the reflection coefficients, the weighting function, $W(a,M)$, has to take into account the geometrical spreading compensation. In the following definitions, indexes S and G are related to source and receiver, respectively.

In this migration scheme, the travel-time curve is located in the 3D space (x, h, t), where x is the mid-point coordinate, h is the half-offset between source and receiver and t is time in the input domain. It is described by 3 parameters – migration dip, α, reflection angle, g, and time in the output domain, t_m. Given a point $M(y,z)$ in the migrated domain, a smooth RMS velocity field, $v(M)$, and a fixed reflection angle, g, (Figure 1) one can calculate the travel-time $t = (l_s + l_g)/v$ using sine and cosine rules. The variation of the migration dip, a, implies in different half-offset between points S and G. As half-offset is not previously defined CMP coordinate has to be calculated as well. Equations (2) provide the parametrical form for the KCATM travel-time curve (Fomel and Prucha, 1999).

$$t = t_m \frac{\cos(a)\cos(g)}{\cos^2(a) - sen^2(g)} \qquad (2a);$$

$$h = \frac{vt_m}{2} \frac{sen(g).\cos(g)}{\cos^2(a) - sen^2(g)} \qquad (2b);$$

$$x - y = \frac{vt_m}{2} \frac{sen(a).\cos(a)}{\cos^2(a) - sen^2(g)} \qquad (2c).$$

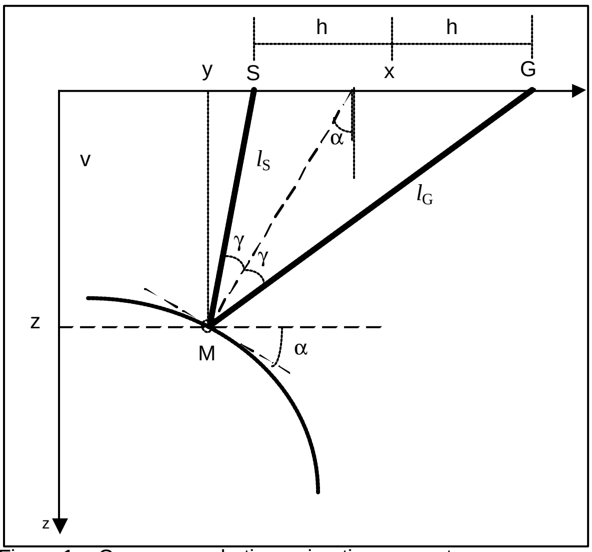

Figure 1 – Common-angle time migration geometry

From equations (2) arises a drawback of the common-angle migration comparing to common-offset migration: the need to load all data in memory to be accessed by the 3D curve, τ_D. Once t_m is the migrated time in the output domain, z and vt_m/2 are interchangeable.

To determine the true amplitude weighting function, $W(a,M)$, the starting point is the general formula (Martins et al., 1997)

$$W_{DS}^{2.5D}(x,M)=\overline{L_S L_G}\sqrt{s_S+s_G}\left(\frac{v^2}{2\cos^2 g}\bar{h}_B\right), \qquad (3)$$

where, $\overline{L_S}$ and $\overline{L_G}$ are the in-line geometrical spreading correction factor; σ_S and σ_G are the out of acquisition plane geometrical spreading correction factor; and $\bar{h}_B$ is the 2D-Beylkin determinant defined as

$$\bar{h}_B = \det\begin{pmatrix} \nabla\tau_{DS} \\ \frac{\partial}{\partial x}\nabla\tau_{DS} \end{pmatrix} = \det\begin{pmatrix} \boldsymbol{p}_S+\boldsymbol{p}_G \\ \frac{\partial}{\partial x}(\boldsymbol{p}_S+\boldsymbol{p}_G) \end{pmatrix} \qquad (4)$$

The Beylkin determinant can be expressed in terms of the unit vector, ***v***, normal to the migration dip at point M. The sum of the slowness vectors $\boldsymbol{p}_S$ and $\boldsymbol{p}_G$ is a normal vector to the reflector at M and can be written as

$$\boldsymbol{p}_S+\boldsymbol{p}_G = \frac{2\cos\gamma}{v}\boldsymbol{v} \qquad (5)$$

and ***v*** is given by

$$\boldsymbol{v} = (\cos\alpha, \sin\alpha) \qquad (6)$$

From equations (5) and (6) follows that

$$\frac{\partial}{\partial x}(\boldsymbol{p}_S+\boldsymbol{p}_G) = \frac{2\cos\gamma}{v}\frac{\partial\alpha}{\partial x}(-\sin\alpha, \cos\alpha) \qquad (7)$$

By substituting the results of equation (7), one obtains for the Beylkin determinant the expression

$$\bar{h}_B = \frac{4\cos^2 g}{v^2}\det\begin{pmatrix} \cos a & \sin a \\ -\frac{\partial a}{\partial x}\sin a & \frac{\partial a}{\partial x}\sin a \end{pmatrix} = \frac{4\cos^2 g}{v^2}\frac{\partial a}{\partial x}$$

(8)

Considering that the velocity *v* can satisfactorily represent an equivalent media above point M, elemental trigonometric rules to determine l_S and l_G, equation (8) and the variable transformation $(\partial a/\partial x)dx = da$, true amplitude weighting function, $W(a,M)$, assumes the form

$$W(a,M)=\frac{v}{2}\frac{\sqrt{t_m^3\cos a.\cos g}}{(\cos^2 a - \sin^2 g)}. \qquad (9)$$

Up to now we provided equations for the stacking line and true amplitude weighting function. In the next section we discuss how to determine the migration aperture and, in turn, the acquisition parameter requirements in order to get true and cheaper amplitudes.

Migration aperture

While submitting a migration job, geophysicists have few parameters to set up. Ideally, some tests, in which they analyze S/N_{mig} and spatial resolution, are run before final migration. One of the tested parameters is migration aperture that controls the extent of the migration operator. According to some authors (Schleicher et al, 1997; Sun, 1998 and 2000; Hertweck et al, 2004) to obtain a properly migrated image – dynamically well migrated – it's necessary to satisfy the following condition

$$|t_D - t_R| < \frac{n\mathrm{T}_w}{2}. \qquad (10)$$

In this equation, τ_D is diffraction time, τ_R is the reflection time (at vicinity of the stationary point) and T_w is an estimative of the wavelet length. The condition in (10) defines the nth order Fresnel Zone radius. In case of KCATM Fresnel zone radius can be expressed as (Guerra et al, 2005)

$$FZ_{(n)} = \frac{v}{2}\sqrt{\frac{n\mathrm{T}_w t_m}{\cos(q)\cos^3(g)}} \qquad (11)$$

where, n is the order of the Fresnel Zone and *q* is the reflector dip angle. Once defined the size of the Fresnel Zone, is necessary to project it onto the measurement surface to determine which traces will be selected to contribute to the output migrated amplitude. This projection has to take into account the desired configuration. So, given a fixed reflection angle, γ, points M and M_n define, on the measurement surface, points x and x – spatial CMP coordinates of the contributing traces. This leads to (Guerra et al, 2005)

$$FZ^{*}_{(n)} = \frac{v}{2}\frac{\sqrt{n\mathrm{T}_w t_m \cos(q)\cos(g)}}{\cos^2(q)-\sin^2(g)} \quad (12)$$

So, given an expected geological dip, q, an estimation of the wavelet length and the desired maximum reflection angle, one can estimate the projected Fresnel Zone which, in turn, summed to the horizontal distance between the stationary point and the migrated point, yields an optimal migration aperture. This horizontal distance can be obtained substituing, in equation 2c, the migration dip, α, by the reflector dip angle, q.

Migration results

To verify the validity of the above calculations, we applied KCATM to a synthetic data modeled with acoustic 2.5D ray tracing on a simple model consisting in a curved reflector separating two half-spaces with velocities 4000m/s (the shallower) and 3000m/s (the deeper) (Figure 2). The offset ranges from 0m to 4000m and shotpoint and receiver interval equals to 10m and it was used a Ricker pulse (15Hz and 125ms length).

The data were submitted to Kirchhoff common offset time migration (KCOTM) and KCATM. Both algorithms are supposed to yield true amplitudes. The migrated amplitudes were picked and compared to the theoretical reflection coefficient for two points indicated by arrows in Figure 2. At the deeper (1500m) – point A – reflector dips around 15^o and at the shallower (1000m) – point B – the dip is 0^o.

Based on the optimum migration aperture described above a 2000m aperture radius is supposed to produce reliable amplitudes up to a 44^o reflection angle at point A and beyond 50^o at point B. Figure 3 shows common angle diffraction curves projected on the h-x plane. The curves show that, considering 2000m aperture radius, is possible to recover true amplitudes only up to 36^o at point A and around 44^o at point B, limited by the maximum offset modeled.

Figures 4 and 5 show KCOTM and KCATM results, respectively, for the migrated point A. In both figures, red line is the theoretical reflection coefficient, green squares are migrated amplitudes and little dots are the normalized difference between theoretical and migrated amplitudes. KCATM recovers true amplitude up to 36^o, as expected. KCOTM yields true amplitude up to the maximum offset that corresponds, based on modeling, to 48^o reflection angle. From these first results, becomes evident that, considering the same offset distribution, KCATM yields true amplitudes to lower angles than KCOTM if the transformation from offset to reflection angle is correct.

To compare the results in the reflection angle domain, KCOTM dataset was transformed to reflection angle assuming a 1D media. Figure 6 shows picked amplitudes and theoretical reflection coefficients versus $\sin^2(\gamma)$ for both migration results, at point A. The differences between curves are evident. For a 15^o dip angle, KCATM amplitudes are closer to the theoretical values than the 1D-reflection-angle-transformed KCOTM ones. The results indicate that, in presence of dip, and using 1D-reflection-angle-transformation for KCOTM data, KCATM is more suitable to AVA amplitude conditioning.

The same analysis was performed to point B. Figure 7 shows that amplitudes were recovered beyond 45^o, as predicted, and the negligible amplitude differences between KCATM and 1D-relfection-angle-transformed KCOTM when dips are gentle.

Conclusions

We discussed some aspects on 2.5D true amplitude common-angle Kircchoff time migration and presented a new acoustic true amplitude weighting function. The analysis of the migration aperture is helpful to get true amplitudes at lower costs. The analysis of the common-angle diffraction curves, in turn, indicates the range of the reflection angle in which migrated amplitudes are reliable. In the same way, these analyses can help to plan acquisition parameters if KCATM is supposed to be applied to the seismic data.

Comparing KCATM and KCOTM we concluded that the former requires more computational effort and larger offsets to obtain true amplitudes at the same reflection angle. AVA curves obtained with KCATM are more reliable than the 1D-reflection-angle-transformed KCOTM in the case of steep dips .

References

Fomel, S., and Prucha, M., 1999, Angle gather time migration. Stanford Exploration Project, Report 100, p.141-151.

Hertweck, T., Jäger, C., Goertz, A., Schleicher, J. , 2004, Aperture effects in 2.5D Kirchhoff migration: A geometrical explanation. Geophysics , 68,.1673-1684,

Guerra, C., Santiago, T., and Tygel, M., 2005, Stationary Kirchhoff common-angle time migration – Aperture definition, submitted to 9th International Congress of the Brazilian Geophysical Society.

Martins, J.M., Schleicher, J., Tygel, M. Santos, L.T., 1997, True-amplitude migration and demigration. Journal of Seismic Exploration, v.6, p.159-180.

Santiago, T, 2004, 2.5D true-amplitude Kirchhoff migration in the common-angle domai. M.Sc Dissertation, Program of Petroleum Science and Engineering, Faculty of Mechanical Engineering, State University of Campinas, Brazil(In Portuguese).

Schleicher, J., Hubral, P., Tygel, M., and Jaya, M. S., 1997, Minimum apertures and Fresnel zones in migration and demigration: Geophysics, 62, 183–194.

Sun, J., 1998, On the limited aperture migration in two dimensions: Geophysics, 63, 984–994.

______, 2000, Limited aperture migration: Geophysics, 65, 584–595.

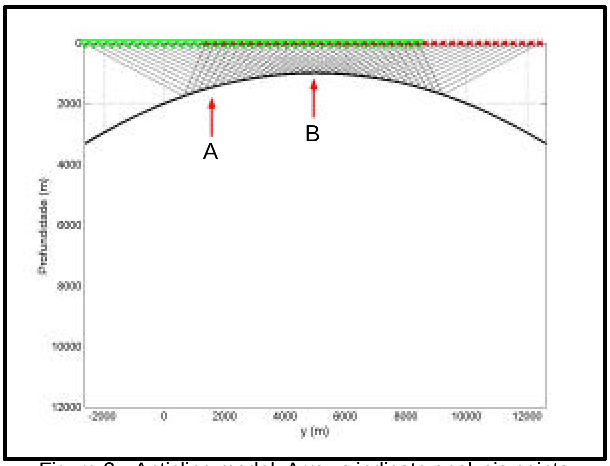

Figure 2 - Anticline model. Arrows indicate analysis points

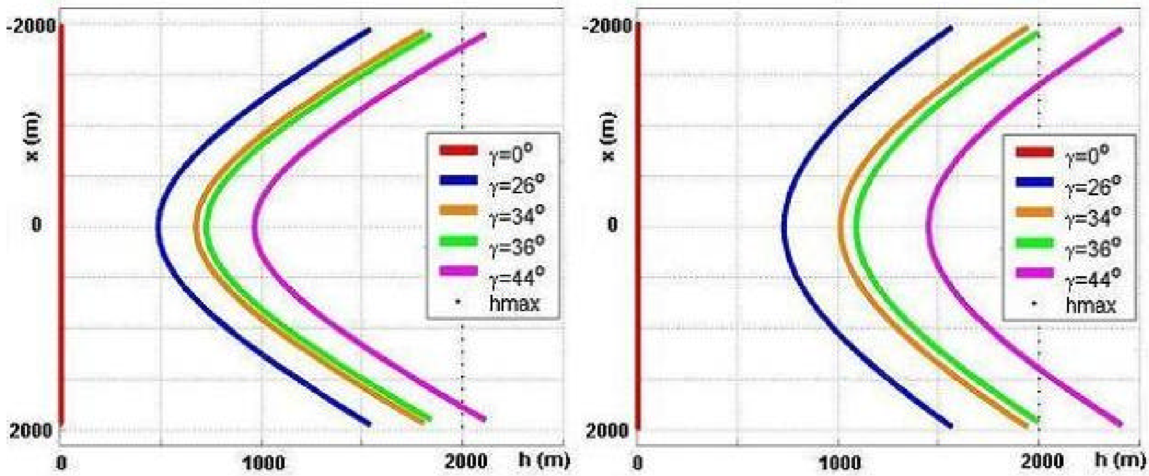

Figure 3 – Diffraction curves projected on x-h plane at points A (right) and B (left).

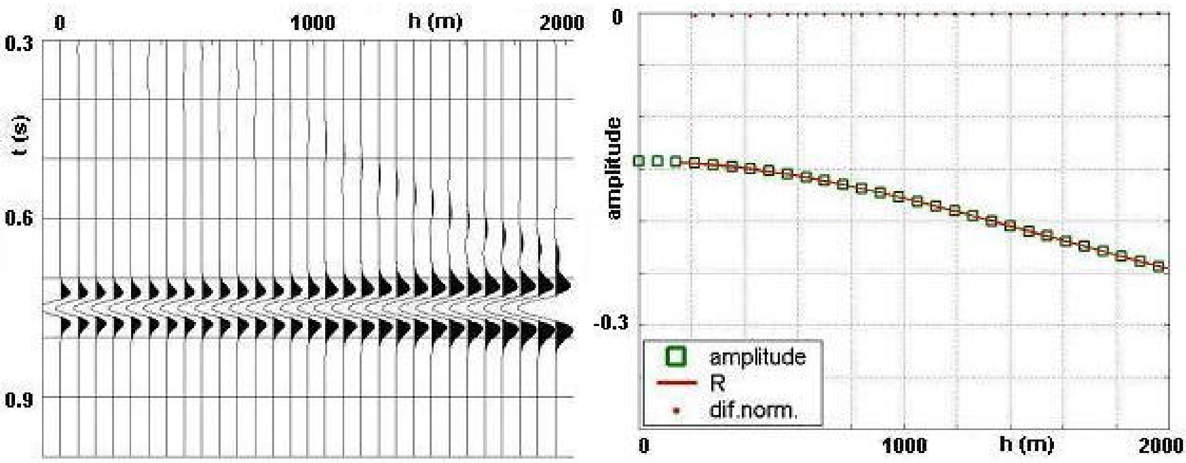

Figure 4 – KCOTM data at point A and corresponding picked amplitudes and modeled reflection coefficients versus half-offset.

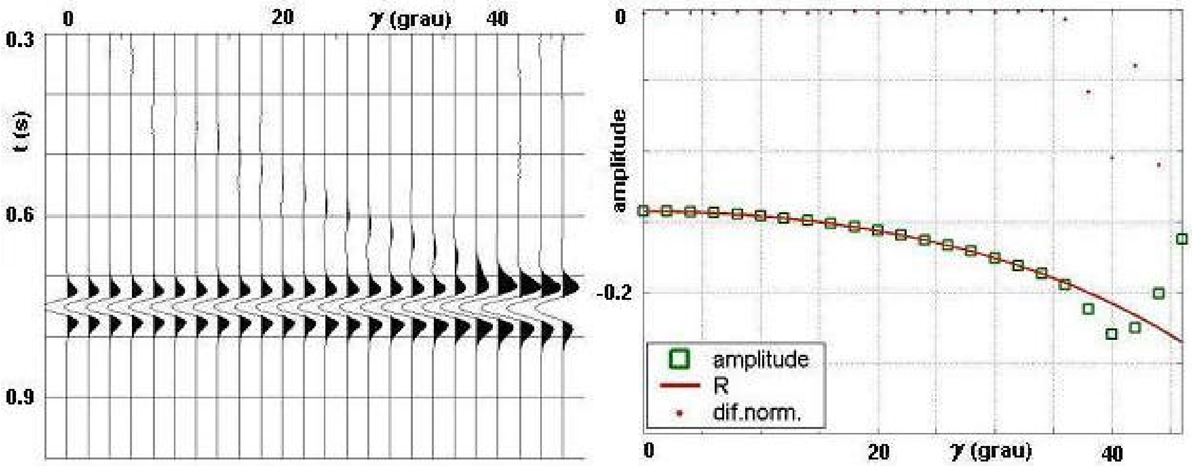

Figure 5 – KCATM data at point A and corresponding picked amplitudes and modeled reflection coefficients versus reflection angle.

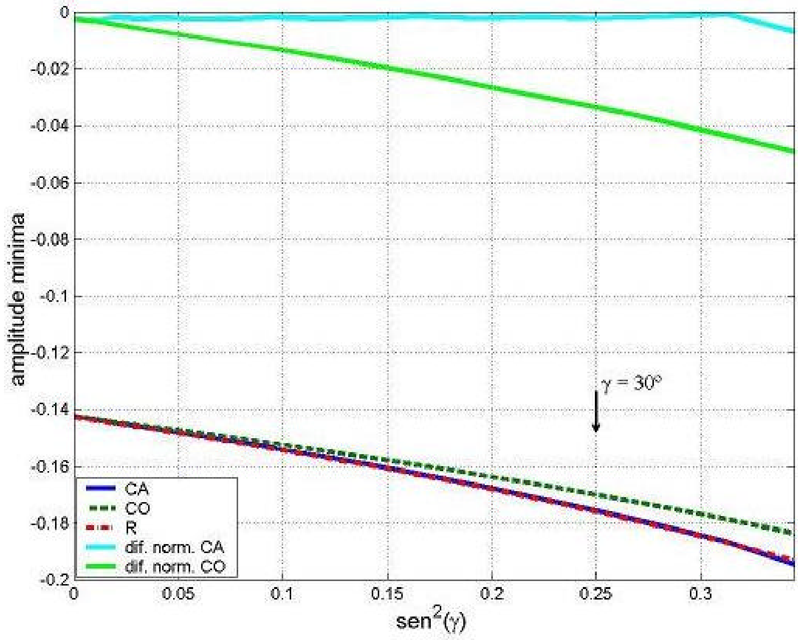

Figure 6 – Picked amplitudes at point A. Dark blue line is referred to KCATM amplitudes and dark green to KCOTM. Light blue is referred to normalized difference between KCATM amplitudes and theoretical reflection coefficient and light green is normalized difference between KCOTM amplitudes and theoretical reflection coefficient.

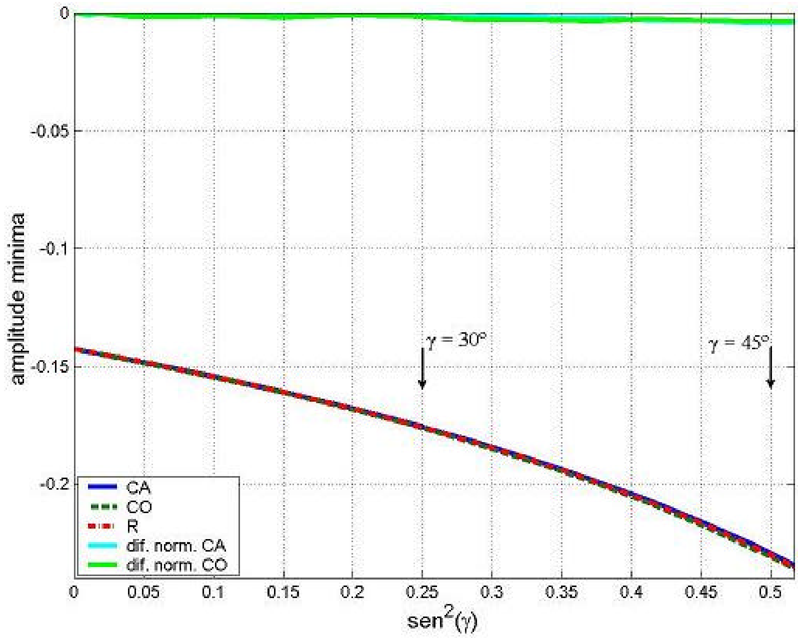

Figure 7 – Picked amplitudes at point B. Dark blue line is referred to KCATM amplitudes and dark green to KCOTM. Light blue is referred to normalized difference between KCATM amplitudes and theoretical reflection coefficient and light green is normalized difference between KCATM amplitudes and theoretical reflection coefficient.